
Article:
Drummond, R. orcid.org/0000-0002-2586-1718, Couto, L.D. orcid.org/0000-0001-8415-7459 and Zhang, D. orcid.org/0000-0002-7945-2100 (2022) Resolving Kirchhoff's laws for parallel Li-ion battery pack state-estimators. IEEE Transactions on Control Systems Technology, 30 (5). pp. 2220-2227. ISSN 1063-6536

https://doi.org/10.1109/tcst.2021.3134451

Resolving Kirchhoff's laws for parallel Li-ion battery pack state-estimators

Ross Drummond, Luis D. Couto and Dong Zhang

***Abstract*—A state-space model for Li-ion battery packs with parallel connected cells is introduced. The key feature of the model is an explicit solution to Kirchhoff's laws for parallel connected packs, which expresses the branch currents directly in terms of the model's states, applied current and cell resistances. This avoids the need to solve these equations numerically. To illustrate the potential of the proposed model for pack-level control and estimation, a method to bound the error of a state-estimator is introduced and the modelling framework is generalised to a class of electrochemical models. It is hoped that the insight brought by this model formulation will allow the wealth of results developed for series connected packs to be applied to those with parallel connections.**

***Index Terms*—Li-ion battery packs, parallel connections, nonlinear state-estimators.**

Introduction

To address ever increasing energy and power demands, Li-ion battery pack sizes are growing rapidly, especially for large-scale applications such as electric vehicles and grid storage. In some parts of the world, it is now common to see electric vehicles powered by thousands of cells, like the Tesla Model S [3], and large batteries, like the planned 50 MW hybrid battery pack to be run near Oxford by Pivot Power [1], are now coming online to support the grid. The sheer number of cells in large battery packs introduces several challenges that need to be overcome such as scalability, cell-to-cell variations, and resilience to component failure [15]. This is especially true for the design of the battery management system (BMS), however, as pack sizes continue to grow, ensuring that the BMS algorithms remain both accurate and scalable enough to be implemented on embedded hardware is becoming ever more challenging, as explored in [12] within the context of the battery model identification problem for example.

Battery models are the foundations for any advanced BMS and to perform at its best, it is desirable for the BMS to have information about every cell in the pack. This has motivated significant efforts to develop models for whole battery packs. However, whilst most large battery packs used in practice are mixtures of both parallel and series connections, most studies on pack level modelling and BMS design are restricted to just series connections, for example [17], [23]. Focusing explicitly on series connected cells greatly simplifies the problem, as every cell in series carries the same current but neglects the diverse spectrum of pack configurations seen in practice.

Whilst including parallel connections into the pack can bring many benefits, such as increased reliability [3] and natural self-balancing [23], modelling and supervising parallel connected cells has proven to be more challenging than cells in series. This is primarily because the branch currents passing through each parallel branch have to be computed at each time instant in the models. The branch currents are obtained by computing solutions to Kirchhoff's laws, making the pack models differential algebraic equation models (DAEs). DAE models can be significantly more complex than those described by ordinary differential equations (ODEs), and often require specialised solvers with short step-sizes to compute valid solutions [19]. As such, most modelling studies on parallel packs numerically compute solutions to Kirchhoff's laws before projecting the state of the index-1 DAE down into an ODE. The fact that parallel pack models are index-1 DAEs is shown here from the unique solution to Kirchoff's laws. Examples of this numerical approach include the iterative scheme of [6], the frequency domain approximations of [5] and the numerical matrix inversion methods of studies like [22] and [4] which was augmented with a thermal model in [14]. In contrast, this work obtains an ODE model by providing an analytical solution to Kirchhoff's laws for n-cells connected parallel. Thus, the main result of this work can be thought of as providing an analytical expression for the parallel pack branch currents in terms of the various cell resistances and model states, negating the need to solve for these currents numerically as done in benchmark studies like (20) of [22] and (15) of [4]. This work then follows along a recent direction in the battery pack modelling literature, including the cell merging approach of [9], and generalises similar efforts like [11], [13] by relaxing some of the restrictive modelling assumptions, like the linearity of the open cell voltage [11], as well as providing a more involved model formulation that additionally includes the important state-of-charge dynamics than [13]. With a state-space formulation for the parallel connected Li-ion battery pack in hand, the state-estimator design problem can then be addressed, with simple gain conditions given

Ross Drummond is with the Department of Engineering Science, University of Oxford, 17 Parks Road, OX1 3PJ, Oxford, United Kingdom. Email: ross.drummond@eng.ox.ac.uk.

Luis D. Couto is with the Department of Control Engineering and System Analysis, Université libre de Bruxelles, Brussels, B-1050, Belgium. Email: lcoutome@ulb.ac.be.

Dong Zhang is with the Department of Mechanical Engineering, Carnegie Mellon University, 5000 Forbes Avenue, Pittsburgh, PA 15312, United States. Email: dongzhr@cmu.edu.

The first author would like to thank the Royal Academy of Engineering for funding through a UKIC fellowship. The second author would like to thank the Wiener-Anspach Foundation for financial support.

in Section III.

Contribution: To be specific, the main contribution of this paper is to introduce a state-space model for parallel connected packs that is fully described by an ordinary differential equation explicitly parameterised by the various resistances and capacitances of the pack's cells. To achieve this, an analytic solution to the algebraic equation of Kirchhoff's laws is stated (see Section II). With this equation in hand, the parallel pack model can then be condensed into a state-space form with an appealing structure that can be exploited for analysis. To illustrate this point, it is shown how the approach can be generalised to a class of electrochemical models and how the state-estimator error for the nonlinear pack dynamics can be bounded.

The results presented here are in many ways an extension of the recent results of [22] from some of the authors but with a focus towards gaining insight about the underlying DAE pack model dynamics. As just one illustration of the potential of this approach, by solving the DAE models' algebraic equations it means that the estimator design conditions of [22, Theorem 3] can now be posed as algebraic inequalities of the pack model parameters, instead of the general state-space formulation posed in [22, Theorem 3]. Additionally, the results show how to extend the parallel pack model to the case when the cell dynamics are described by a certain class of electrochemical models and how to optimise the worst-case bound for the state-estimator error. It is hoped that the analysis presented in this paper will lead to new results in other applications where parallel pack models are used, for example in determining the weakest cells in the packs, detecting thermal runaway and enabling whole pack state-estimators for large Li-ion battery packs.

Notation: If a square matrix A of dimension n is positive definite then $A \in \mathbb{S}^n_{\succ 0}$ and if it is negative definite then $A \in \mathbb{S}^n_{\prec 0}$. More generally, if a matrix A is negative-definite then $A \prec 0$. If A is a non-negative diagonal matrix then $A \in \mathbb{D}^n_+$. The identity matrix of dimension n is denoted I_n and the matrix of zeros of dimension $m \times n$ is denoted $\mathbf{0}_{n\times m}$. A signal x is said to belong to a Hilbert space $x \in \mathcal{L}_2$ if the norm $\|x\|_2 = \sqrt{\int_0^\infty x(t)^2\, dt}$ is bounded.

I. DAE model for a parallel connected pack

In this section, the equations of a DAE model for Li-ion batteries connected in parallel are briefly described, with the equations now standard. In Section II, this DAE model is converted into an ODE by resolving the underlying algebraic equation for the branch currents.

A. Parallel pack model equations

Figure 1 shows the set-up of the parallel connected Li-ion battery pack to be modelled. While this work focuses exclusively on parallel connected packs, it is expected that, after some minor reformulation, the presented results may be readily generalised to other pack configurations that combine cells connected in series and parallel, following the results of [10] and others.

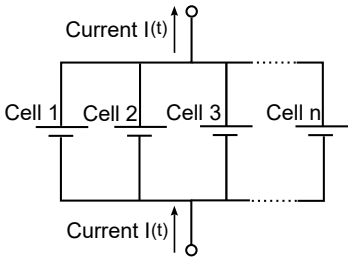

Figure 1: A Li-ion battery pack containing n cells connected in parallel.

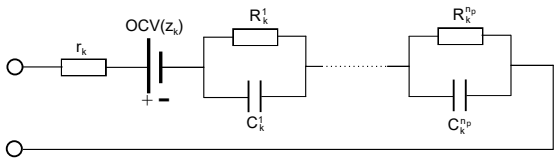

Figure 2: Equivalent circuit model for the battery dynamics. Here, r_k is the k^{th} cell's series resistance, $\text{OCV}(z_k)$ is its open circuit voltage and $(R_k^\ell,\, C_k^\ell)$ with $\ell = 1, \ldots, n_p$ denote the ℓ^{th} RC-pair.

Each cell is assumed to be described by the equivalent circuit model of Figure 2, composed of a nonlinear voltage source (for the open circuit voltage which maps the state-of-charge), n_p RC pairs and the series resistance r_k. The RC pairs approximate solid-state diffusion within the active material particles and lead to notably simpler dynamics than the fractional systems associated with Warburg elements. The dynamics of the k^{th} cell in the pack with this circuit model are

$$\dot{x}_k(t) = \bar{A}_k x_k(t) + \bar{B}_k i_k(t), \quad k = 1, \ldots, n, \tag{1a}$$

$$v_k(t) = \sum_{\ell=1}^{n_p} w_k^\ell(t) + \text{OCV}(z_k(t)) + r_k i_k(t), \tag{1b}$$

where $x_k \in \mathbb{R}^{n_k} = [z_k{}^T, w_k{}^T]^T$ is the state-space, $z_k(t) \in [0,1]$ is the state-of-charge of each cell and $w_k(t) \in \mathbb{R}^{n_p} = [w_k{}^1(t), \ldots, w_k^{n_p}(t)]^T$ is the relaxation voltage of cell k composed of elements $w_k^\ell(t)$- the voltage across the ℓ^{th}-RC pair. Throughout, it is assumed that the state dimension of each cell is the same, as in $n_k = n_p + 1,\ \forall k = 1, \ldots, n$, and so the state dimension of the whole pack is $N = n_k n$. The cell voltages $v_k(t)$ (the measured signal) are the sums of the relaxation voltages $w_k(t)$, the open circuit voltage $\text{OCV}(z_k(t))$ and a resistance term from r_k. Because the cells are connected in parallel, each cell voltage is the same, as in $v_k(t) = v(t)\, \forall k = 1, \ldots, n$. The state space matrices in (1) are

$$\bar{A}_k = \begin{bmatrix} 0 & 0 \\ 0 & -\tau_k \end{bmatrix}, \quad \bar{B}_k = \begin{bmatrix} \frac{1}{Q_k} \\ \frac{1}{C_k} \end{bmatrix}, \tag{2}$$

where Q_k is the battery capacity, $\tau_k = \text{diag}(1/(R_k^1 C_k^1), \ldots, 1/(R_k^{n_p} C_k^{n_p})) \in \mathbb{D}^{n_p}_+$ contains the

time constants and $1/C_k = [1/C_k^1, \ldots, 1/C_k^{n_p}]^T \in \mathbb{R}^{n_p}$ with C_k^j the capacitance of the j^{th} RC-pair in cell k.

What remains is to compute the branch current i_k going into each cell. This is done by applying Kirchhoff's laws to the circuit model (1). Namely, Kirchhoff's voltage law implies for cells $j, k \in \{1, 2, \ldots, n\}$ that

$$\text{OCV}(z_j) + \sum_{\ell=1}^{n_p} w_j^\ell + r_j i_j = \text{OCV}(z_k) + \sum_{\ell=1}^{n_p} w_k^\ell + r_k i_k, \tag{3a}$$

and the current law states that the sum of the currents going into each branch $i_k(t)$ equals the pack current $I(t)$

$$\sum_{k=1}^{n} i_k(t) = I(t). \tag{3b}$$

In this work, the convention that a positive current charges the cell is adopted.

B. Differential algebraic equation parallel pack model

When combined, the dynamic circuit equations (1) and the algebraic equations for Kirchhoff's laws (3) can be collected into a single DAE system [22],

$$\begin{bmatrix} I_N & \mathbf{0}_{N\times n} \\ \mathbf{0}_{n\times N} & \mathbf{0}_{n\times n} \end{bmatrix} \begin{bmatrix} \dot{x}(t) \\ \dot{i}(t) \end{bmatrix} = \begin{bmatrix} A_{11} & A_{12} \\ A_{21} & A_{22} \end{bmatrix} \begin{bmatrix} x(t) \\ i(t) \end{bmatrix} + \begin{bmatrix} \mathbf{0}_{N\times 1} \\ \phi(t) \end{bmatrix} \tag{4}$$

where $A_{11} = \text{diag}(\bar{A}_1, \bar{A}_2, \ldots, \bar{A}_n)$, $A_{12} = \text{diag}(\bar{B}_1, \bar{B}_2, \ldots, \bar{B}_n)$, $S = \begin{bmatrix} 0 & -\mathbf{1}_{n_p}{}^T \end{bmatrix}$,

$$A_{22} = \begin{bmatrix} r_1 & -r_2 & 0 & \ldots & 0 \\ r_1 & 0 & -r_3 & \ddots & \vdots \\ \vdots & \vdots & \ddots & \ddots & 0 \\ r_1 & 0 & \ldots & 0 & -r_n \\ 1 & 1 & 1 & \ldots & 1 \end{bmatrix}, \tag{5a}$$

$$A_{21} = \begin{bmatrix} 0 & \mathbf{1}_{n_p}{}^T & S & \mathbf{0}_{1\times n_p} & \ldots & \mathbf{0}_{1\times n_p} \\ 0 & \mathbf{1}_{n_p}{}^T & \mathbf{0}_{1\times n_p} & S & \ddots & \vdots \\ \vdots & \vdots & \vdots & \ddots & \ddots & \mathbf{0}_{1\times n_p} \\ 0 & \mathbf{1}_{n_p}{}^T & \mathbf{0}_{1\times n_p} & \ldots & \mathbf{0}_{1\times n_p} & S \\ 0 & 0 & \mathbf{0}_{1\times n_p} & \ldots & \mathbf{0}_{1\times n_p} & \mathbf{0}_{1\times n_p} \end{bmatrix}, \tag{5b}$$

and

$$\phi(t) = \begin{bmatrix} \text{OCV}(z_1) - \text{OCV}(z_2) \\ \vdots \\ \text{OCV}(z_1) - \text{OCV}(z_n) \\ I(t) \end{bmatrix}. \tag{5c}$$

The variables with a time derivative $x(t) = [x_1(t)^T, \ldots, x_n(t)^T]^T$ are known as the *differential* or state-space variables whilst the branch current vector $i(t) = [i_1(t), \ldots, i_n(t)]^T$ is the model's *algebraic* variable. The branch currents are obtained by solving

$$i(t) = -A_{22}{}^{-1} \left(A_{21} x(t) + \phi(t) \right), \tag{6}$$

given that the matrix A_{22} is invertible (as shown in Section II). Substituting the expression for the currents (6) into the DAE model (4) reduces it to an ODE

$$\dot{x}(t) = (A_{11} - A_{12} A_{22}{}^{-1} A_{21}) x(t) - A_{12} A_{22}{}^{-1} \phi(t). \tag{7}$$

II. Resolving the algebraic equation

The main results of this paper are contained in this section where an algebraic solution for the current going into each branch of the parallel circuit is obtained. In this way, the parallel connected pack model of Section I can be fully characterised as an algebraic expression of the pack cell resistances and the model states $x(t)$.

A. The matrix inverse $A_{22}{}^{-1}$

The main stumbling block behind resolving the algebraic equation (6) for the branch currents is determining the matrix inverse $A_{22}{}^{-1}$. In the following theorem, an analytic expression for this matrix inverse is stated.

Theorem 1: Consider the matrix A_{22} in (5a) with positive resistances $r_i > 0$ for $i = 1, \ldots, n$. Then $A_{22}{}^{-1} = m$ where m is a matrix composed of elements $m_{j,k}$ satisfying

$$m_{k,n} = \frac{1}{r_k \sum_{\ell=1}^{n} \frac{1}{r_\ell}}, \quad k = 1, \ldots, n, \tag{8a}$$

$$m_{k,j} = \frac{1}{r_k r_{j+1}} \left(\sum_{\ell=1}^{n} \frac{1}{r_\ell} \right)^{-1}, \ j = 1, \ldots, n-1, \quad \& \, k \neq j+1, \tag{8b}$$

$$m_{k,k-1} = \frac{1}{{r_k}^2} \left(\sum_{\ell=1}^{n} \frac{1}{r_\ell} \right)^{-1} - \frac{1}{r_k}, \ k = 2, 3, \ldots, n. \tag{8c}$$

Proof. The problem can be cast as finding the unique solution to

$$A_{22} m = I_n, \tag{9}$$

whose expanded form is given in (10) at the top of the following page.

Multiplying through by the row of 1's in A_{22} gives the following relations for the column sums of m

$$\sum_{\ell=1}^{n} m_{\ell,k} = 0, \quad \forall k \neq n, \tag{11a}$$

$$\sum_{\ell=1}^{n} m_{\ell,n} = 1, \tag{11b}$$

and, similarly, multiplying through by the other rows implies, for $k = 2, \ldots n$,

$$r_1 m_{1,j} = r_k m_{k,j}, \quad j = 1, \ldots, n, \, j \neq k-1, \tag{12a}$$

$$r_1 m_{1,k-1} = 1 + r_k m_{k,k-1}. \tag{12b}$$

Relating (12a) for different j and k implies

$$m_{\ell,j} = \frac{r_k}{r_\ell} m_{k,j}, \ j = 1, \ldots, n, \ k \neq j+1, \, \ell \neq j+1, \quad \& \ k = 2, \ldots, n, \ \ell = 2, \ldots, n. \tag{13}$$

From these relations, the n^{th} column of m can be extracted. Starting from (11b) and substituting in (13)

$$\sum_{\ell=1}^{n} \frac{r_k}{r_\ell} m_{k,n} = 1, \quad k = 1, 2, , \ldots, n, \tag{14}$$

$$\begin{bmatrix} r_1 & -r_2 & 0 & \dots & 0 \\ r_1 & 0 & -r_3 & \ddots & \vdots \\ \vdots & \vdots & \ddots & \ddots & 0 \\ r_1 & 0 & \dots & 0 & -r_n \\ 1 & 1 & \dots & 1 & 1 \end{bmatrix} \begin{bmatrix} m_{1,1} & m_{1,2} & \dots & \dots & m_{1,n} \\ m_{2,1} & m_{2,2} & \dots & \dots & m_{2,n} \\ \vdots & \vdots & \vdots & \vdots & \vdots \\ m_{n-1,1} & m_{n-1,2} & \dots & \dots & m_{n-1,n} \\ m_{n,1} & m_{n,2} & \dots & \dots & m_{n,n} \end{bmatrix} = \begin{bmatrix} 1 & 0 & \dots & 0 & 0 \\ 0 & 1 & \ddots & \ddots & 0 \\ \vdots & \ddots & \ddots & \ddots & \vdots \\ 0 & \ddots & \ddots & 1 & 0 \\ 0 & 0 & \dots & 0 & 1 \end{bmatrix} \tag{10}$$

gives the the n^{th} column of m,

$$m_{k,n} = \frac{1}{r_k \sum_{\ell=1}^{n} \frac{1}{r_\ell}}, \quad k = 1, 2, \dots, n. \tag{15}$$

To compute the remaining elements of m, it is noted that (12b) implies

$$m_{k,k-1} = \frac{r_1 m_{1,k-1} - 1}{r_k}, \quad k = 2, 3, \dots, n. \tag{16}$$

Substituting (12a) and (16) into (11a) gives for $k = 2, 3, \dots, n$

$$\sum_{\ell=1, \ell \neq k+1}^{n} \frac{r_1}{r_\ell} m_{1,k-1} + \frac{r_1 m_{1,k-1} - 1}{r_k} = 0. \tag{17}$$

In other words,

$$m_{1,k-1} = \left(\sum_{\ell=1}^{n} \frac{1}{r_\ell} \right)^{-1} \frac{1}{r_1 r_k}, \quad k = 2, 3, \dots, n. \tag{18}$$

The remaining elements of m are then obtained from (12a) and (16). ■

B. State-space model

With the matrix ${A_{22}}^{-1}$ inverse defined, an explicit solution for the ODE model (7) can be stated. To arrive at this statement, several matrices and vectors first have to be established. Defining the vector of open-circuit and relaxation voltages as

$$\text{OCV}(z(t)) = \begin{bmatrix} \text{OCV}(z_1(t)) \\ \vdots \\ \text{OCV}(z_n(t)) \end{bmatrix}, \; w_\Sigma(t) = \begin{bmatrix} \sum_{\ell=1}^{n_p} w_1^\ell \\ \vdots \\ \sum_{\ell=1}^{n_p} w_n^\ell \end{bmatrix}, \tag{19}$$

then the solution to the branch current equation (6) can be expressed as

$$i(t) = \Pi_v (\text{OCV}(z(t)) + w_\Sigma(t)) + \Pi_I I(t) \tag{20}$$

where

$$\Pi_v = - \begin{bmatrix} \sum_{i=1}^{n-1} m_{1,i} & -m_{1,1} & -m_{1,2} & \dots & -m_{1,n-1} \\ \vdots & \vdots & \vdots & \vdots & \vdots \\ \sum_{i=1}^{n-1} m_{i,n} & -m_{n,1} & -m_{n,2} & \dots & -m_{n,n-1} \end{bmatrix}, \tag{21a}$$

$$\Pi_I = - \begin{bmatrix} m_{1,n}, & \dots, & m_{n-1,n}, & m_{n,n} \end{bmatrix}^T. \tag{21b}$$

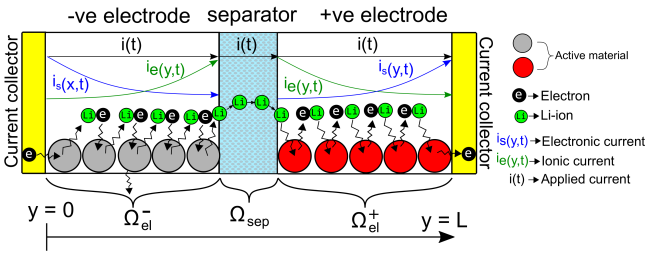

Figure 3: Domain of the DFN electrochemical model. Also illustrated is the charge transfer mechanism and ionic/electronic current distributions of the model.

Next, the vector of concatenated voltages is defined

$$\check{v}(t) = \mathbf{1}_n v(t) = \begin{bmatrix} \sum_{\ell=1}^{n_p} w_1^\ell(t) + \text{OCV}(z_1(t)) + r_1 i_1(t) \\ \vdots \\ \sum_{\ell=1}^{n_p} w_n^\ell(t) + \text{OCV}(z_n(t)) + r_n i_n(t) \end{bmatrix}. \tag{22}$$

Using the substitution (20), this voltage vector of repeating elements can be formulated as

$$\check{v}(t) = Cx(t) + D_{\text{OCV}} \text{OCV}(z(t)) + D_I I(t), \tag{23}$$

where $C = (I_n + \boldsymbol{r}\Pi_v)W$ with $\boldsymbol{r} = \text{diag}(r_k)$, $k = 1, \dots, n$, $W \in \mathbb{R}^{n \times N}$ is defined by $w_\Sigma(t) = Wx(t)$, $D_{\text{OCV}} = I_n + \boldsymbol{r}\Pi_v$ and $D_I = \boldsymbol{r}\Pi_I$.

With these matrices defined, the dynamics of (7) can be written as

$$\dot{x}(t) = Ax(t) + B_{\text{OCV}} \text{OCV}(z(t)) + B_I I(t), \tag{24}$$

where $A = A_{11} - A_{12}{A_{22}}^{-1}A_{21}$ with $A_{12}{A_{22}}^{-1}A_{21} = \bar{B}\Pi_v W$, $B_{\text{OCV}} = \bar{B}\Pi_v$ and $B_I = \bar{B}\Pi_I$ where $\bar{B} = A_{12}$.

Two key features of the parallel equivalent circuit pack model are i) it is an ODE whose vector field is written explicitly in terms of the circuit parameters (the various resistance and capacitances), and ii) the model nonlinearities (from the open circuit voltages OCVs) enter in an affine manner. With the added assumption that these OCVs are slope-restricted, then this nonlinear circuit model can be thought of as a Lurie system [8], [21], a class of nonlinear systems whose analysis is tractable.

C. Extension to electrochemical models

Whilst the results so far have focussed on the simple RC circuit models of Figure 2, the method of solving for the branch currents can be generalised to more complex

electrochemical battery models with linear series resistances, such as the Doyle-Fuller-Newman (DFN) model [7]. To show this, consider the cell set-up of Figure 3 with the voltage defined as the difference in the solid-phase potential $\phi_{\rm s}(y,t)$ at either current collector- with spatial variable $y \in [0,\, L]$ and the solid-phase composed of the active material and conducting carbon. By defining the electrode potential $\phi_{\rm el}(y,t) = \phi_s(y,t) - \phi_{\rm e}(y,t)$ as the difference between the solid-phase potential and that of the electrolyte $\phi_{\rm e}(y,t)$, this voltage expression can be expressed as

$$\begin{aligned} v(t) &= \phi_{\rm s}(L,t) - \phi_{\rm s}(0,t) + r_{\rm ct} i(t), \qquad (25)\\ &= \phi_{\rm el}(L,t) + \int_{\Omega_{\rm el}^+} \frac{\partial \phi_{\rm e}(y,t)}{\partial y}\, dy + \int_{\Omega^{\rm sep}} \frac{\partial \phi_{\rm e}(y,t)}{\partial y} dy \\ &\quad + \int_{\Omega_{\rm el}^-} \frac{\partial \phi_{\rm e}(y,t)}{\partial y} dy - \phi_{\rm el}(0,t) + r_{\rm ct} i(t), \qquad (26) \end{aligned}$$

where $\Omega_{\rm el}^+$ is the domain of the positive electrode, $\Omega_{\rm el}^-$ is that of the negative electrode, $\Omega_{\rm sep}$ is the domain of the separator and $r_{\rm ct}$ is the contact resistance.

Within the framework of the DFN electrochemical model [7], in each electrode, these potentials are obtained by solving, for cell $k = 1, , \ldots, n$,

$$i_{\rm e}(y,t) = \kappa^{\pm}(y,t) \frac{\partial \phi_{\rm e}(y,t)}{\partial y} + \theta^{\pm}(y,t) \frac{\partial \ln\, c_e(y,t)}{\partial y}, \quad (27a)$$

$$i_{\rm s}(y,t) = \sigma^{\pm}(y,t) \frac{\partial \phi_{\rm s}(y,t)}{\partial y}, \quad (27b)$$

$$i_k(t) = i_{\rm s}(y,t) + i_{\rm e}(y,t), \quad (27c)$$

where (27a) is Ohm's law for the ionic current $i_e(y,t)$, (27b) is Ohm's law for the electronic current $i_{\rm s}(y,t)$ and (27c) enforces current conservation. For the sake of simplifying the notation, the subscript k identifying the equations for cell k was dropped from the electrochemical terms in these equations. Furthermore, here, $\sigma^{\pm}(y,t)$ is the electronic conductivity, $\kappa^{\pm}(y,t)$ is the ionic conductivity, $\theta^{\pm}(y,t)$ accounts for the contribution to the ionic current from the build-up of bulk electrolyte and $\pm$ indicates whether the domain is the positive or negative electrode. Manipulating the current conservation equation (27c)

$$\begin{aligned} i_k(t) &= \sigma^{\pm}(y,t) \frac{\partial \phi_{\rm el}(y,t)}{\partial y} + (\kappa^{\pm}(y,t) + \sigma^{\pm}(y,t)) \frac{\partial \phi_{\rm e}(y,t)}{\partial y} \\ &\quad + \theta^{\pm}(y,t) \frac{\partial \ln\, c_e(y,t)}{\partial y} \qquad (28) \end{aligned}$$

allows the electrolyte potential gradient in each electrode to be expressed as

$$\frac{\partial \phi_{\rm e}(y,t)}{\partial y} = \frac{i_k(t) - \sigma^{\pm}(y,t) \frac{\partial \phi_{\rm el}(y,t)}{\partial y} - \theta^{\pm}(y,t) \frac{\partial \ln\, c_e(y,t)}{\partial y}}{\kappa^{\pm}(y,t) + \sigma^{\pm}(y,t)}. \quad (29)$$

Similarly, in the separator, where there is no electronic current as electrons do not flow across it, then

$$\frac{\partial \phi_{\rm e}(y,t)}{\partial y} = \frac{i_k(t) - \theta^{\rm sep}(y,t) \frac{\partial \ln\, c_e(y,t)}{\partial y}}{\kappa^{\rm sep}(y,t)} \quad (30)$$

where superscript sep indicates parameters for the separator.

Plugging these relations back into (26) gives the cell voltage expression

$$v_k(t) = f_k(\phi_{\rm el}(y,t), c_{\rm e}(y,t), t) + r_k\, i_k(t), \quad (31)$$

where $f_k(\phi_{\rm el}(y,t), c_{\rm e}(y,t), t)$ is an integral function taking the place of the $\text{OCV}(z_k) + \sum_{\ell=1}^{n_p} w_k^{\ell}$ term of the equivalent circuit voltage (1b) and

$$\begin{aligned} r_k = &\int_{\Omega_{\rm el}^+} \frac{1}{\kappa^+(y,t) + \sigma^+(y,t)}\, dy + \int_{\Omega_{\rm sep}} \frac{1}{\kappa^{\rm sep}(y,t)}\, dy \\ &+ \int_{\Omega_{\rm el}^-} \frac{1}{\kappa^-(y,t) + \sigma^-(y,t)}\, dy + r_{\rm ct} \qquad (32) \end{aligned}$$

is the series resistance of the cell. To ensure that the DFN model's voltage (31) has no nonlinear resistance term emerging from resolving the algebraic variables, $f_k(\phi_{\rm el}(y,t), c_{\rm e}(y,t), t)$ is imposed to be a function of the model's differential states only. Applying this condition ensures the numerical solver for the model simulation can evaluate (31), and hence Kirchoff's laws, directly at each time step. Since the branch currents enter the DFN model voltage via $r_k i_k(t)$, just like in the equivalent circuit voltage (1b), the same methodology of computing the branch currents can be applied as in Sections II-A and II-B. To express (31) in terms of differential variables, it is necessary to obtain a time derivative of the electrode potential $\phi_{\rm el}$, as the bulk electrolyte c_e is a differential state since it is driven by diffusion [7]. Electrode potential dynamics are included within DFN model by accounting for fast double-layer capacitance effects [8], [18], converting the divergence equation of the DFN model into

$$C_{\rm dl}^{\pm} \frac{\partial \phi_{\rm el}(y,t)}{\partial t} = \frac{\partial i_e(y,t)}{\partial y} - a_s^{\pm} F j(y,t) \quad (33)$$

where $C_{\rm dl}^{\pm}$ is the specific capacitance, $a_s^{\pm}$ is the reacting surface area, F is Faraday's constant, $j(y,t)$ are Butler-Volmer reaction kinetics and the ionic current flux is expressed in terms of the differential variables from (27a) and (29).

With the voltage expression (31) in hand, and using the simplified notation $f_k(.) = f_k(\phi_{\rm el}(y,t), c_{\rm e}(y,t), t)$ for the model states' contribution to the voltage, Kirchoff's voltage law from (3a) becomes

$$f_j(.) + r_j i_j(t) = f_k(.) + r_k i_k(t) \quad (34)$$

for cells $j, k \in \{1, \ldots, n\}$. Notice the similarity of this expression to (3a), with a series resistance multiplying the current and another (nonlinear) term accounting for the contribution from the models' differential states. By having a similar structure, the same reasoning as used in Theorem 1 can be applied to compute the branch currents for the DFN model, giving

$$i(t) = \Pi_v f(.) + \Pi_I I(t) \quad (35)$$

where $f(.) = [f_1(.), \ldots, f_n(.)]^T$ and the matrices Π_v and Π_I have the same structure as (21) but are built from the

resistances of (32). The current distribution across n DFN electrochemical models in parallel can then be computed from the model states c_e and ϕ_{el} and applied current $I(t)$.

In the above, the fact that the DFN model incorporates the cell's nonlinear resistance within the Butler-Volmer reactions kinetics, instead of the series resistance r_k, was exploited. However, this feature does not hold for all electrochemical models, most notably it does not hold for the single particle model [20] where spatially averaged- and hence linear- reaction kinetics are used which leads to a nonlinear series resistance from the overpotential. Approximate solutions obtained after linearising this nonlinear resistance may then have to be considered for computing the parallel branch currents with such models.

III. State estimator error bounds

Returning to the equivalent circuit pack model of (1), the value of the proposed method for evaluating pack-level current distributions illustrated by introducing a method to bound the error of a state-estimator. The pack is taken to be subject to the nonlinear dynamics of (24) and external disturbances on its current $d_I \in \mathcal{L}_2$ and voltage $d_v \in \mathcal{L}_2$. Current disturbances $d_I(t)$ are assumed instead of additive disturbances acting on the state vector field to ensure there is no violation of Kirchhoff's laws at any time. Defining the perturbed current as $\tilde{I}(t) = I(t) + d_I(t)$ then the battery model plant becomes

$$\dot{x}(t) = Ax(t) + B_{\text{OCV}}\text{OCV}(z(t)) + B_I\tilde{I}(t), \tag{36a}$$
$$\check{v}(t) = Cx(t) + D_{\text{OCV}}\text{OCV}(z) + D_I\tilde{I}(t) + \mathbf{1}_n d_v(t). \tag{36b}$$

The following state-estimator is proposed for this system

$$\dot{\hat{x}}(t) = A\hat{x}(t) + B_{\text{OCV}}\text{OCV}(\hat{z}(t)) + B_I I(t) - K(\check{v}(t) - \check{\hat{v}}(t)) \tag{37}$$

with $\hat{x}(t) = [\hat{z}_k(t)^T, \hat{w}_k(t)^T]^T$, $k = 1, \ldots, n$ being the estimated states composed of the estimated state-of-charge $\hat{z}_k(t)$ and relaxation voltages $\hat{w}_k(t)$, $\check{\hat{v}}(t)$ is the predicted voltage, $\hat{i}_k(t)$ are the estimator's currents, $K \in \mathbb{R}^{n\times N}$ is the known estimator gain and

$$\check{\hat{v}}(t) = \begin{bmatrix} \hat{v}(t) \\ \vdots \\ \hat{v}(t) \end{bmatrix} = \begin{bmatrix} \sum_{\ell=1}^{n_p} \hat{w}_1^\ell(t) + \text{OCV}(\hat{z}_1(t)) + r_1\hat{i}_1(t) \\ \vdots \\ \sum_{\ell=1}^{n_p} \hat{w}_n^\ell(t) + \text{OCV}(\hat{z}_n(t)) + r_n\hat{i}_n(t) \end{bmatrix}, \tag{38a}$$
$$= C\hat{x}(t) + D_{\text{OCV}}\text{OCV}(\hat{z}(t)) + D_I I(t), \tag{38b}$$

the voltage concatenation.

Defining the error between the plant (36) and the state estimator (37) as $e(t) = x(t) - \hat{x}(t)$ then the error dynamics can be written

$$\dot{e}(t) = Ae(t) + B_{\text{OCV}}\Delta\text{OCV}(t) + K(\check{v}(t) - \check{\hat{v}}(t)), \tag{39}$$

where ΔOCV is the open circuit voltage error

$$\Delta\text{OCV}(t) = \text{OCV}(z(t)) - \text{OCV}(\hat{z}(t)). \tag{40}$$

Using the voltage definitions of the plant (36b) and the estimator (38b), these dynamics can be expressed as

$$\dot{e}(t) = (A + KC)e(t) + (B_{\text{OCV}} - KD_{\text{OCV}})\Delta\text{OCV}(t) + KD_I d_I(t) + K\mathbf{1}_n d_v(t), \tag{41a}$$
$$= A_e e(t) + B_{e,\text{OCV}}\Delta\text{OCV}(t) + B_{e,I}d_I(t) + B_{e,v}d_v(t). \tag{41b}$$

With these dynamics, the state-estimator error can be bounded by solving the following semi-definite programme, a class of convex optimisation problems for which many solvers now exist.

Proposition 1: If there exists $P \in \mathbb{S}^N_{\succ 0}$, $\gamma = \text{diag}(\gamma_I, \gamma_v) \in \mathbb{D}^2_+$, $\tau \in \mathbb{D}^n_+$, matrices

$$M = \begin{bmatrix} PA_e + \frac{1}{2}I_N & PB_{e,\text{OCV}} & P[B_{e,I},\, B_{e,v}] \\ \mathbf{0}_{n\times 2} & \mathbf{0}_{n\times n} & \mathbf{0}_{n\times N} \\ \mathbf{0}_{2\times N} & \mathbf{0}_{2\times n} & -\frac{1}{2}\gamma \end{bmatrix}, \tag{42a}$$

$$\Omega = \begin{bmatrix} -\underline{\delta}\overline{\delta}Z^T\tau Z & \frac{1}{2}(\overline{\delta} + \underline{\delta})Z^T\tau & \mathbf{0}_{N\times 2} \\ \frac{1}{2}(\overline{\delta} + \underline{\delta})\tau Z & -\tau & \mathbf{0}_{n\times 2} \\ \mathbf{0}_{2\times N} & \mathbf{0}_{2\times n} & \mathbf{0}_{2\times 2} \end{bmatrix}, \tag{42b}$$

where $Z \in \mathbb{R}^{n\times N}$ is defined by $z(t) = [z_1(t), \ldots, z_n(t)]^T = Zx(t)$ and $\overline{\delta}$, $\underline{\delta}$ are the OCV slope bounds

$$\frac{d\text{OCV}(z_k(t))}{dz_k(t)} = \delta \in [\underline{\delta}, \overline{\delta}], \quad \underline{\delta} > 0,\ \forall z_k(t) \in [\underline{z}, \overline{z}] \tag{43}$$

which solves

$$\min\ V(e(0)) + \gamma_I\|d_I\|_2^2 + \gamma_v\|d_v\|_2^2, \tag{44a}$$
$$\text{subject to } M + M^T + \Omega \prec 0, \tag{44b}$$

then the estimator error is bounded by

$$\|e\|_2^2 \le V(e(0)) + \gamma_I\|d_I\|_2^2 + \gamma_v\|d_v\|_2^2 \tag{45}$$

for all $d_I, d_v \in \mathcal{L}_2$ where $V(e(t)) = e(t)^T Pe(t)$.

Proof. Define $\xi(t) = [e(t)^T, \Delta\text{OCV}(t)^T, d_I(t), d_v(t)]^T$ and note that

$$\xi^T(t)\Omega\xi(t) = \left(\overline{\delta}Ze(t) - \text{OCV}(t)\right)^T \tau\left(\text{OCV}(t) - \underline{\delta}Ze(t)\right) \ge 0, \tag{46}$$

from the OCV slope-bounds of (43). Consider the storage function $V(e(t)) = e(t)^T Pe(t)$ and note that multiplying (44b) on the left by $\xi(t)^T$ and on the right by $\xi(t)$ gives

$$\frac{dV(e(t))}{dt} + e(t)^T e(t) + \xi^T\Omega\xi - \gamma_I {d_I}^2 - \gamma_v {d_v}^2 \le 0. \tag{47}$$

Applying the S-procedure [21] and exploiting the positivity of the slope-restriction inequality (46), then (47) implies

$$\frac{dV(e(t))}{dt} + e(t)^T e(t) \le \gamma_I {d_I}^2 + \gamma_v {d_v}^2. \tag{48}$$

Integrating from $t = 0$ to $t = T$ gives

$$\|e\|_2^2 \le V(e(0)) - V(e(T)) + \gamma_I\|d_I\|_2^2 + \gamma_v\|d_v\|_2^2 \tag{49}$$

with the bound (45) then holding since $V(e(T)) \ge 0$. ■

Remark 1: One approach to set the estimator gain K is to define it as the Kalman gain of a linearised point of the error dynamics, as widely adopted in practice and as considered in the numerical simulations of Section IV. ⋆

	$k=1$	$k=2$	$k=3$
a_k	5.6495	2.9993	6.903×10^3
b_k	0.4	0.4	4
c_k	0.4922	2.6829	3.2585
ζ_k	0.1	0.9	//

Table I: Parameters for the OCV curve in (51).

Remark 2: Since Propositions 1 is derived from results on absolute stability theory and Lurie systems [21], it is robust in the sense that the bound holds for all OCV curves satisfying the slope restriction of (51). Robustness to un-modelled dynamics may also be achieved in a similar way, for example, by representing the ℓ^{th} RC-pair time constants as

$$\frac{1}{R_k^\ell C_k^\ell} = \frac{1}{\bar{R}_k^\ell \bar{C}_k^\ell} + \Delta_{RC}^\ell(t) \tag{50}$$

where $\Delta_{RC}^\ell(t) \in [0, \overline{\Delta}_{RC}^\ell]$ is a norm bounded disturbance and $\bar{R}_k^\ell \bar{C}_k^\ell$ are the nominal values. The uncertainty in $\Delta_{RC}^\ell(t)$ could then be incorporated within the analysis using a sector-type inequality as adopted for the OCV slope-restriction of (43). $\star$

IV. Simulations

The presnted results are now evaluated through numerical simulations of a parallel connected pack. Consider 2.1Ah Li-ion cells ($LiFePO_4$ cathodes and graphite anodes) connected in parallel such that, for cells $k = 1, 2, \ldots, n$, the capacitances are $Q_k = 2.1 \times 3600$, $C_k = 2250$ and the resistances are Gaussian, as in $r_k \sim \mathcal{N}(0.0175, 0.001)$, $R_k \sim \mathcal{N}(0.01, 0.001)$. The mean parameter values were obtained from [16] by assuming a one RC-pair model ($n_p = 1$) and isothermal conditions at 25°C. The OCV for this cell was also measured in [16] using a C/20 cycling test and is reproduced in Figure 4a. The following fit is proposed for this OCV curve

$$\text{OCV}(z_k) = \begin{cases} a_1 {z_k}^{b_1} + c_1, & 0 \le z_k, \le \zeta_1, \\ a_2(z_k - \zeta_1)^{b_2} + c_2, & \zeta_1 < z_k < \zeta_2, \\ a_3(z_k - \zeta_2)^{b_3} + c_3, & \zeta_2 \le z_k \le 1, \end{cases} \tag{51}$$

which is compared to the measured data of [16] in Figure 4a using the parameters of Table I, giving a reasonable fit. Clearly, since $a_k > 0$ and $b_k > 0$ for each $k = 1, 2, 3$, this OCV curve is a monotonic function of the state-of-charge z_k and so the OCV slope restriction assumption of (51) holds.

The parallel pack model was driven by a scaled version of the combined Artemis drive cycle (CADC) [2] shown in Figure 4b. In the following, this current is referred to as $I_{\text{drive}}(t)$. The initial conditions of the plant were $w_k(0) = 0$, $z_k(0) = 0.1$ for $k = 1, 2, \ldots, n$. Figure 4c shows the deviation in the branch current of the first parallel branch from the average when $n = 3$, highlighting the heterogeneous charging of the cells in the pack. The variation between the branch currents in this simulation suggests that, if the cells' parameters vary, and as cells age any variation should amplify, then they will carry different currents which could lead to thermal and degradation hotspots in the pack.

Figure 5 examines the performance of a state-estimator for the parallel pack model driven by the drive cycle current. Two situations were considered, one where the estimator gain K was the Kalman gain linearised around a state-of-charge of 0.5 (the simulations were found to be quite robust to this linearisation point) and the other being the standard implementation of the extended Kalman filter (EKF). For the simulations, the current and voltage disturbances were Gaussian $d_I(t) = \mathcal{N}(0, n)$, $d_v(t) = \mathcal{N}(0, 1)$. Simulations for various different pack sizes were considered, with $n = 3, 5, 10, 15, 20$. To normalise the simulations against the number of cells in the pack, the applied current was scaled by $I(t) = n \times I_{\text{drive}}(t)$. The initial conditions of the estimator were $\hat{w}(0) = 0$ and the initial state-of-charge error was set to be the unique value such that its square equalled 0.1 but its sum equalled zero, as in

$$\sum_{k=1}^{n} (z_k(0) - \hat{z}_k(0))^2 = 0.1, \quad \sum_{k=1}^{n} z_k(0) - \hat{z}_k(0) = 0. \tag{52}$$

The performance of the state-estimator measured by the 2-norm of the error is shown in Figure 5. With the normalisations discussed above, the exponential convergence rates of the estimators were found to be roughly independent of the number of cells in the pack, but the steady-state error generally increased with the number of cells, although the error was small for all packs considered. Moreover, no significant performance benefits were observed with the EKF, which implies that strong justifications have to be made for implementing an EKF over a standard Kalman filter as the EKF was found to be more computationally demanding to simulate. For the 3-cell pack, the bound of Proposition 1 was $\gamma_v = 2.34 \times 10^{-4}$, $\gamma_I = 75.48$ and $(\hat{x}(0) - x(0))^T P(\hat{x}(0) - x(0)) = 36.38$, with this bound holding for the nonlinear dynamics, albeit conservatively.

Conclusions

A state-space model for lithium-ion battery packs connected in parallel was introduced. The key result of the paper was a solution to Kirchhoff's laws for parallel connected packs which allowed the various branch currents charging each cell to be written explicitly in terms of the pack's state-space variables, applied current and the various cell resistances. In this way, the model avoided the need to compute these branch currents numerically. This result was then extended to a class of electrochemical model such that current distributions in a parallel pack with Doyle-Fuller-Newman cell models could be obtained. A method to compute bounds for pack-level state-estimator errors was also presented.

References

[1] *https://www.pivot-power.co.uk/press-release/oxford-kickstarts-ev-revolution-with-energy-superhub-oxford/.* Accessed 18/02/21.

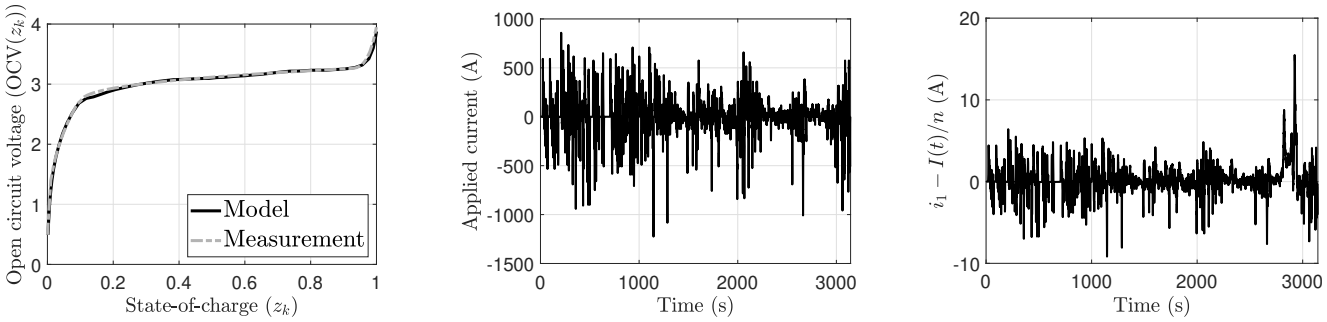

(a) Open circuit voltage. (b) Scaled Artemis drive current. (c) Branch current variation.

Figure 4: OCV curve, applied current ($I(t) = I_{\text{drive}}(t)$) and deviation in the branch current of cell 1 from the average.

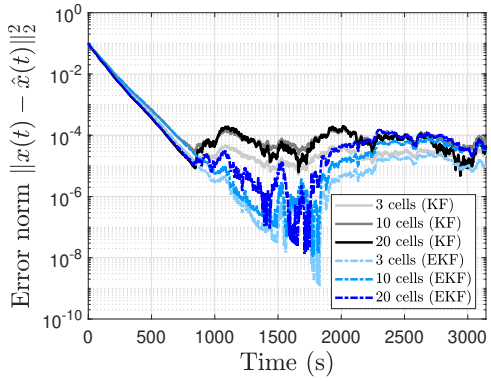

Figure 5: Comparison between the standard (grey) and extended (blue) Kalman filter error for parallel connected packs of various sizes.

[2] M. André, "The ARTEMIS european driving cycles for measuring car pollutant emissions," *Science of the Total Environment*, vol. 334, pp. 73–84, 2004.

[3] M. J. Brand, M. H. Hofmann, M. Steinhardt, S. F. Schuster, and A. Jossen, "Current distribution within parallel-connected battery cells," *Journal of Power Sources*, vol. 334, pp. 202–212, 2016.

[4] T. Bruen and J. Marco, "Modelling and experimental evaluation of parallel connected lithium ion cells for an electric vehicle battery system," *Journal of Power Sources*, vol. 310, pp. 91–101, 2016.

[5] L. Chang, C. Zhang, T. Wang, Z. Yu, N. Cui, B. Duan, and C. Wang, "Correlations of cell-to-cell parameter variations on current and state-of-charge distributions within parallel-connected lithium-ion cells," *Journal of Power Sources*, vol. 437, p. 226869, 2019.

[6] W. Diao, M. Pecht, and T. Liu, "Management of imbalances in parallel-connected lithium-ion battery packs," *Journal of Energy Storage*, vol. 24, p. 100781, 2019.

[7] M. Doyle, T. F. Fuller, and J. Newman, "Modeling of galvanostatic charge and discharge of the lithium/polymer/insertion cell," *Journal of the Electrochemical society*, vol. 140, no. 6, p. 1526, 1993.

[8] R. Drummond, A. M. Bizeray, D. A. Howey, and S. R. Duncan, "A feedback interpretation of the Doyle-Fuller-Newman lithium-ion battery model," *IEEE Transactions on Control Systems Technology*, 2019.

[10] A. Fill, S. Koch, and K. P. Birke, "Analytical model of the current distribution of parallel-connected battery cells and strings," *Journal of Energy Storage*, vol. 23, pp. 37–43, 2019.

[9] X. Fan, W. Zhang, Z. Wang, F. An, H. Li, and J. Jiang, "Simplified battery pack modeling considering inconsistency and evolution of current distribution," *IEEE Transactions on Intelligent Transportation Systems*, 2020.

[11] A. Fill, S. Koch, A. Pott, and K.-P. Birke, "Current distribution of parallel-connected cells in dependence of cell resistance, capacity and number of parallel cells," *Journal of Power Sources*, vol. 407, pp. 147–152, 2018.

[12] A. Fotouhi, D. J. Auger, K. Propp, and S. Longo, "Accuracy versus simplicity in online battery model identification," *IEEE Transactions on Systems, Man, and Cybernetics: Systems*, vol. 48, no. 2, pp. 195–206, 2016.

[13] M. H. Hofmann, K. Czyrka, M. J. Brand, M. Steinhardt, A. Noel, F. B. Spingler, and A. Jossen, "Dynamics of current distribution within battery cells connected in parallel," *Journal of Energy Storage*, vol. 20, pp. 120–133, 2018.

[14] E. Hosseinzadeh, J. Marco, and P. Jennings, "Combined electrical and electrochemical-thermal model of parallel connected large format pouch cells," *Journal of Energy Storage*, vol. 22, pp. 194–207, 2019.

[15] H. Kim and K. G. Shin, "Efficient sensing matters a lot for large-scale batteries," in *Procs. of the Second International Conference on Cyber-Physical Systems*. IEEE, 2011, pp. 197–205.

[16] X. Lin, H. E. Perez, S. Mohan, J. B. Siegel, A. G. Stefanopoulou, Y. Ding, and M. P. Castanier, "A lumped-parameter electro-thermal model for cylindrical batteries," *Journal of Power Sources*, vol. 257, pp. 1–11, 2014.

[17] X. Lin, A. G. Stefanopoulou, Y. Li, and R. D. Anderson, "State of charge imbalance estimation for battery strings under reduced voltage sensing," *IEEE Transactions on Control Systems Technology*, vol. 23, no. 3, pp. 1052–1062, 2014.

[18] I. J. Ong and J. Newman, "Double-layer capacitance in a dual lithium ion insertion cell," *Journal of The Electrochemical Society*, vol. 146, no. 12, p. 4360, 1999.

[19] L. Petzold, "Differential/algebraic equations are not ode's," *SIAM Journal on Scientific and Statistical Computing*, vol. 3, no. 3, pp. 367–384, 1982.

[20] S. Santhanagopalan and R. E. White, "Online estimation of the state of charge of a lithium ion cell," *Journal of power sources*, vol. 161, no. 2, pp. 1346–1355, 2006.

[21] M. Vidyasagar, *Nonlinear systems analysis*. SIAM, 2002.

[22] D. Zhang, L. D. Couto, S. Benjamin, W. Zeng, D. F. Coutinho, and S. J. Moura, "State of charge estimation of parallel connected battery cells via descriptor system theory," in *Procs. of the American Control Conference*, 2020, pp. 2207–2212.

[23] L. Zhong, C. Zhang, Y. He, and Z. Chen, "A method for the estimation of the battery pack state of charge based on in-pack cells uniformity analysis," *Applied Energy*, vol. 113, pp. 558–564, 2014.